Pin-Loaded Holes in Large Orthotropic Plates

P. D. Mangalgiri*
Indian Institute of Science, Bangalore, India

Pin-loaded holes commonly occur in engineering structures. However, accurate analysis of such holes presents formidable difficulties because of the load-dependent contact of the pin with the plate. Significant progress has recently been achieved in the analysis of holes in isotropic plates. This paper develops a simple and accurate method for the partial contact analysis of pin-loaded holes in composites. The method is based on an inverse formulation that seeks to determine loads in a given contact-separation configuration. A unified approach for all types of fit was used. Continuum solutions were obtained for infinitely large plates of various typical orthotropic properties with holes loaded by smooth rigid pins. These solutions were then compared with those for isotropic plates. The effects of orthotropy and the type of fit were studied through load-contact relationships, distribution of stresses and displacements, and their variation with load. The results are of direct relevance to the analysis and design of pin joints in composite plates.

Nomenclature

a	= radius of the hole
a_{ij}	= compliance coefficients for the material
C	= contact region
$C_0, C_1, C_2, \ldots$	= free constants in the Fourier expansion for radial stress at the hole boundary
E	= Young's modulus in the direction of the load
E_1, E_2	= Young's moduli in two principal directions of the orthotropy
e	$= \beta_1\beta_2 = \sqrt{E_1/E_2}$
G_{12}	= shear modulus for the orthotropic material
h_1, h_2	= material parameters defined as $h_j = -[(\nu_{12}\beta_j/E_1) + 1/E_2\beta_j]$
i	$= \sqrt{-1}$
n	$= \beta_1 + \beta_2 = [2(e - \nu_{12}) + E_1/G_{12}]^{1/2}$
P, Q, R	= material parameters as defined in the text
P_x	= load per unit thickness applied at the pin in X direction
$(P_x)_{th}$	= threshold value of P_x at which separation initiates in interference fits
$r, \theta; x, y$	= polar and Cartesian coordinates relative to hole center
S	= separation region
U, V	= radial and tangential displacements
u, v	= displacements in Cartesian coordinates
u_R	= rigid-body displacement between pin and the plate
z	$= x + iy$
z_1, z_2	= transformed variables defined by $z_j = x + \mu_j y$
β_1, β_2	= material parameters as defined in text
$\phi_1(z_1), \phi_2(z_2)$	= complex potentials for stress field in the orthotropic plate
λ	= proportional interference (pin diameter − hole diameter)/hole diameter (takes negative values for clearance)
μ_1, μ_2	= roots of characteristic equation, given by $\mu_j = i\beta_j$
ν_{12}	= Poisson's ratio for orthotropy for axes 1-2
ζ_j	= transformed variables defined by $\zeta_j = z_j + \sqrt{z_j^2 - a^2(1+\mu_j^2)}/a(1 - i\mu_j)$
σ	= direct or shear stress with proper subscripts
$2\theta_c, 2\theta_s$	= arcs of contact and separation, respectively
$2\theta_p$	= arc of separation for push fit

Received June 15, 1983; revision received Feb. 8, 1984.

*Senior Scientific Officer, Department of Aerospace Engineering (presently, NRC Research Associate, NASA Langley Research Center, Hampton, Va.).

Introduction

PIN-LOADED holes occur often in engineering structures—they constitute a basic mechanism of load transfer from one structural component to another. Although continuously bonded joints are favored for composites, joints using a pin-hole combination (pin joints) become indispensable in many situations. This is particularly so in the case of articulated joints and joints needing repeated assembly and disassembly. The load transfer in a practical pin joint can be considered to be made up of two basic load systems:

1) Plate load in which a self-equilibrating load is applied at the edges of the plate, with no net load on the pin.

2) Pin load in which the load transfer takes place from the pin to the plate, the load applied at the pin reacting at the edges of the plate.

The case of plate load was analyzed in an earlier paper.[1] Here we analyze the case of pin load. However, in both cases the unbonded nature of the pin-plate interface gives rise to the important aspect of the problem, i.e., that the contact area may depend upon the load. This is obviously so for clearance fit pins. But, even in the case of interference fit joints, with the increase in the load the initial compressive stress may be relieved at certain point(s) and the pin may separate from the plate; with a further increase in the load, the contact is only partial and depends upon the load. This feature, the partial load-dependent contact, leads to moving boundary conditions and consequent nonlinearity in the problem. The anisotropy of composites further complicates the problem. Because of this, analytical attempts to accurately estimate the stresses and deformations around pin-loaded holes with due regard to partial contact have been few and sporadic in the past, even for isotropic plates.[2-5] A good review of earlier partial contact work in isotropic plates can be found in Ref. 6. In the last few years, significant success has been achieved in the analysis of the partial contact problems of the pin joints.[6-12] This success can be attributed to an inverse formulation in which the nature of the contact zones is predicted beforehand and load levels are sought for a given extent of the contact. Such an approach will also be the basis of the present analysis.

In the case of orthotropic materials, the problem of full contact with the plate load was solved as early as 1945 by Green[13] as a result of an interest in timber structures. However, in spite of the growing interest in fiber-reinforced composites (FRC), the analyses of the pin load case and

partial contact were not achieved until recently. As late as 1977, de Jong[14] proposed an approximate analysis for pin-loaded holes that does not satisfy the interfacial boundary conditions. The only attempts so far to analyze pin-loaded holes in composites that consider partial contact appear to be those by Oplinger and Gandhi.[15,16] They consider only push fit, but are a step ahead in considering the slip in the presence of finite friction. They treat the problem using a complex variable formulation by Lekhnitskii[17] and use an elaborate iterative procedure requiring computational effort on a large scale for matching the zones of contact and separation. Reference 18 uses inverse formulation and is a comprehensive study on pin joints in composites of which the present paper is a part.

The current paper presents theory of elasticity solutions (small deformation) in plane stress for the pin-loaded hole in an infinitely large orthotropic sheet. The pin is assumed to be smooth and rigid. A unified approach for all types of fits is taken. Load-contact behavior, stresses, and deformations are studied for various orthotropic properties typical of the FRC available today.

Basic Configuration and Inverse Formulation

An infinite thin elastic orthotropic plate is considered with a hole of diameter $2a$ as shown in Fig. 1a. The hole in the unloaded plate is filled with a rigid pin of diameter $2a(1+\lambda)$. The parameter λ is called the proportional interference and characterizes the fit of the joint to be either interference ($\lambda>0$), push (neat) ($\lambda=0$), or clearance ($\lambda<0$). The interface is assumed to be smooth and frictionless. The axes of orthotropy are labeled as 1 and 2 and coincide with the reference axes X and Y. E_1 and E_2 are the principal elastic moduli, G_{12} the shear modulus, and ν_{12} Poisson's ratio. Without any loss of generality E_1 is taken to be higher than E_2. The polar coordinates (r,θ) are centered at the center of the pin, U and V denote the displacements in the r and θ directions with respect to the pin, and σ_r, σ_θ, and $\sigma_{r\theta}$ denote the radial, tangential (hoop), and shear stress, respectively. The load P_x is applied to the pin in the X direction, see Fig. 1b. Unless otherwise stated, P_x is taken as the load per unit thickness and has the dimensions of force per unit length. When the load P_x acts along the stiffer axis of orthotropy, the loading will be labeled as case I, the other case (load along weaker axis) being case II. The load P_x is reacted at the edges of the plate in the far field where all the stresses tend to vanish, but their integral over the (infinite) boundary of the plate is equal and opposite to P_x. Let C denote that part of the hole periphery where contact exists between the pin and the plate and S is the remaining part where they are separated. Then $C+S$ denotes the complete hole periphery.

The boundary conditions of the problem are

$$\sigma_{r\theta}=0 \qquad \text{on} \quad C+S \tag{1a}$$

$$U=a\lambda, \quad \sigma_r\le 0 \qquad \text{on} \quad C \tag{1b}$$

$$\sigma_r=0, \quad U\ge a\lambda \qquad \text{on} \quad S \tag{1c}$$

$$a\int_C(\sigma_{r\theta}\sin\theta-\sigma_r\cos\theta)\,d\theta=P_x \tag{1d}$$

$$(\sigma_r,\sigma_\theta,\sigma_{r\theta})\to 0 \quad \text{as} \quad r\to\infty \tag{1e}$$

The peculiar feature of the problem is the appearance of the unilateral constraints in the form of inequalities in the boundary conditions, Eqs. (1b) and (1c). These constraints determine the extents of C and S, which are generally a priori unknown.

From the symmetry of the problem it is obvious that the separation and contact zones must be symmetric about the X axis and the contact zone must be under the load P_x ($\theta=0$). Figure 1b depicts this picture. The contact configuration can be completely described by specifying the angle of the contact $2\theta_c$ or the angle of separation $2\theta_s$. Because of the simplicity in predicting the nature of the contact-separation configuration, the problem can be advantageously formulated in the inverse way as: "Given the configuration of contact and separation (i.e., the angle θ_c or θ_s) and relevant material parameters, what is the level of load P_x required?" When posed in this way, the unilateral constraints are satisfied whenever the equality conditions are satisfied along the entire boundary, including the transition points.[1] Because of the symmetry, it is enough to consider only the upper half of the domain, say, $(0\le\theta\le\pi)$. Angle θ_c specifies the contact zone and angle θ_s specifies the separation zone, if any. Thus, the C and S are specified as

$$C: \qquad 0\le\theta\le\theta_c, \quad r=a$$

$$S: \qquad \theta_c\le\theta\le\pi, \quad r=a$$

Solution

The solution is sought through the determination of complex potentials $\phi_1(z_1)$ and $\phi_2(z_2)$ of the orthotropic field from which stresses and deformations can easily be obtained. Following Lekhnitskii,[17] z_1 and z_2 are the complex variables defined as

$$z_j=x+\mu_j y, \qquad j=1,2 \tag{2}$$

where $\mu_j=i\beta_j$ ($\beta_j\ge 0$) are the roots of the characteristic equation

$$a_{11}\mu^4-2a_{16}\mu^3+(2a_{12}+a_{66})\mu^2-2a_{26}\mu+a_{22}=0 \tag{3}$$

$$a_{11}=1/E_1, \qquad a_{12}=-\nu_{12}/E_1,$$

$$a_{22}=1/E_2, \qquad a_{66}=1/G_{12}, \qquad a_{16}=a_{26}=0 \tag{4}$$

The parameters β_j are given by

$$\beta_j^2=\frac{1}{2}\left[\frac{E_1}{G_{12}}-2\nu_{12}\pm\sqrt{\left(\frac{E_1}{G_{12}}-2\nu_{12}\right)^2-4\frac{E_1}{E_2}}\,\right] \tag{5}$$

with the restriction on the material parameters that

$$\left(\frac{E_1}{G_{12}}-2\nu_{12}\right)\ge 2\sqrt{\frac{E_1}{E_2}}$$

This is not very restrictive since most of the composite materials fall in this category except for a few shear-stiff laminates.

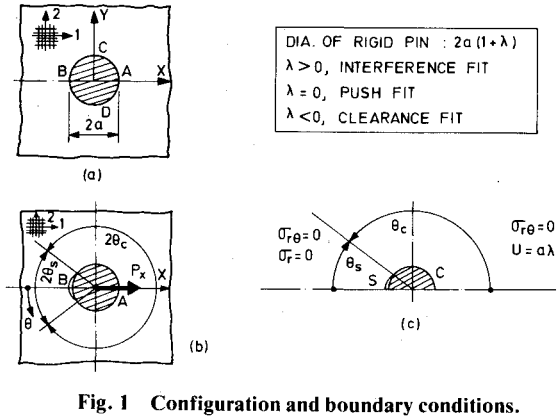

Fig. 1 Configuration and boundary conditions.

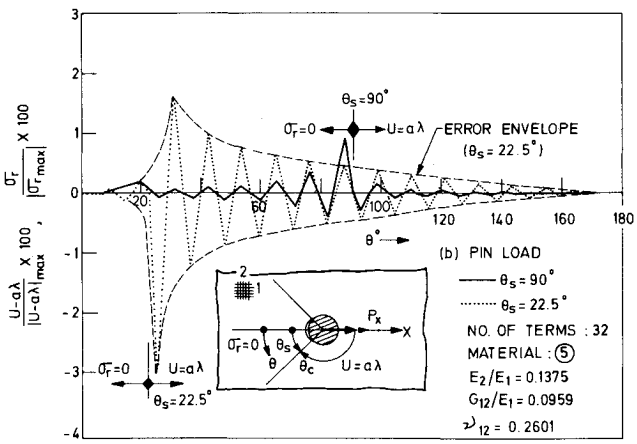

Fig. 2 Error distribution on hole boundary, interference fit.

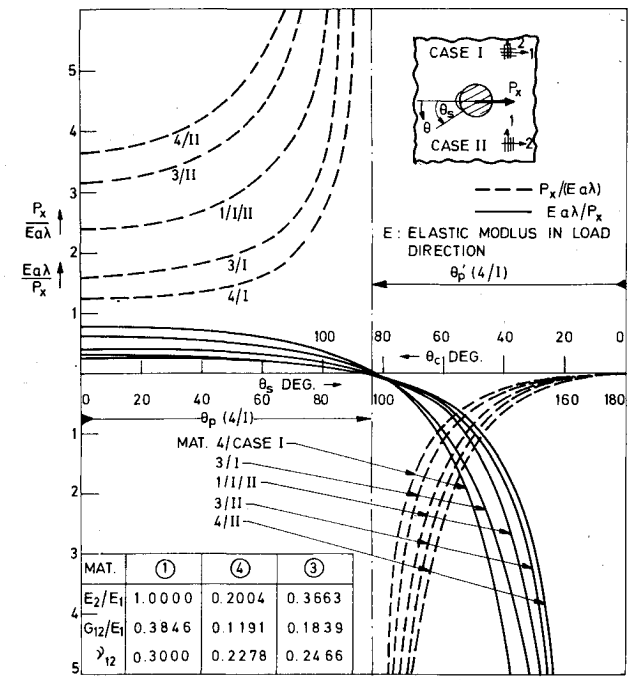

Fig. 3 Pin load vs separation/contact behavior for various orthotropy.

Since the stress state is symmetric about the X axis, the unknown radial stress σ_r on the interface can be put in the Fourier series form as

$$\sigma_r(a,\theta)=\frac{1}{2}C_0+\sum_{m=1,2,3,\ldots}C_m\cos m\theta \tag{6}$$

The shear stress $\sigma_{r\theta}$ all along the interface is known (to be zero). Following Lekhnitskii, the stress potentials satisfying Eqs. (1a), (1d), (1e), and (6) can be obtained as

$$\phi_j(z_j)=\frac{P_x}{4\pi}\frac{h_k}{\beta_j h_k-\beta_k h_j}\ell n\zeta_j+\frac{a}{4}\frac{1-\beta_k}{\beta_j-\beta_k}\frac{1}{\zeta_j}C_0$$
$$+\frac{a}{4}\frac{1-\beta_k}{\beta_j-\beta_k}\frac{1}{2\zeta_j^2}C_1+\frac{a}{4(\beta_j-\beta_k)}\sum_{m=2,3,\ldots}C_m\left[\frac{1-\beta_k}{(m+1)\zeta_j^{m+1}}\right.$$
$$\left.-\frac{1+\beta_k}{(m-1)\zeta_j^{m-1}}\right] \qquad (k=3-j,\quad j=1,2) \tag{7}$$

where

$$h_j=a_{12}\beta_j-a_{22}/\beta_j \tag{8}$$

$$\zeta_j=\frac{z_j+\sqrt{z_j^2-a^2(1+\mu_j^2)}}{a(1-i\mu_j)} \tag{9}$$

The unknown constants C_m and the load P_x are to be obtained so as to satisfy Eqs. (1b) and (1c).

We consider two cases: full contact ($\theta_s=0$) and partial contact ($\theta_s>0$).

Full Contact

Full contact is encountered in interference fits at low levels of load P_x. We obtain expressions for U at $r=a$ from the stress potentials [Eq. (7)] and express the same in the form of a Fourier series. Since $U=a\lambda$ on the entire hole periphery, by equating constant terms to $a\lambda$ and coefficients of $\cos m\theta$ to zero, we get an infinite system of equations as follows:

$$C_1=-P_x/(\pi a)$$

$$RC_0+PC_2=E_1\lambda;\quad E_1u_R/a+(R/2)C_1+(P/2)C_3=0$$

$$\frac{E_1u_R}{a}+(P+R)C_0+\frac{1}{2}(P+R)C_1$$
$$+\sum_{m=2,3,\ldots}^{\infty}C_m\left(\frac{P+R}{m+1}+\frac{P+Q}{m-1}\right)=E_1\lambda$$
$$\frac{P}{m-1}C_{m-2}+\left(\frac{R}{m+1}+\frac{Q}{m-1}\right)C_m+\frac{P}{m+1}C_{m+2}=0 \tag{10}$$

where the constant u_R introduced to permit the rigid-body mode is chosen to make the displacement of the point A (Fig. 1b) equal to $a\lambda$ and the material parameters P, Q, and R are defined as

$$P=n(e-1)/4$$
$$Q=[-n(e+1)+2(\nu_{12}-e)]/4$$
$$R=[-n(e+1)-2(\nu_{12}-e)]/4$$
$$n=\beta_1+\beta_2=[2(e-\nu_{12})+E_1/G_{12}]^{1/2}$$
$$e=\beta_1\beta_2=(E_1/E_2)^{1/2} \tag{11}$$

The system of Eqs. (10) can be solved by terminating the series of Eq. (7) at some finite number of terms $m=M$, so that $C_m=0$ for $m>M$. The convergence can be studied by obtaining solutions for various values of M. Once the constants C_m are evaluated, the stresses and displacements can be obtained through complex potentials ϕ_j.

As the load P_x is increased from zero, the initial compressive radial stress over a part of the periphery is reduced and ultimately the radial stress just vanishes at $\theta=\pi$ at a threshold load $P_x=(P_x)_{\text{th}}$, where separation initiates. The condition $\sigma_r(a,\pi)=0$ gives

$$\frac{1}{2}C_0+\sum_{m=1,2,3,\ldots}C_m(-1)^m=0 \tag{12}$$

Adding this equation to the system of Eqs. (10) and treating $P_x=(P_x)_{\text{th}}$ as unknown, we obtain the value of $(P_x)_{\text{th}}$.

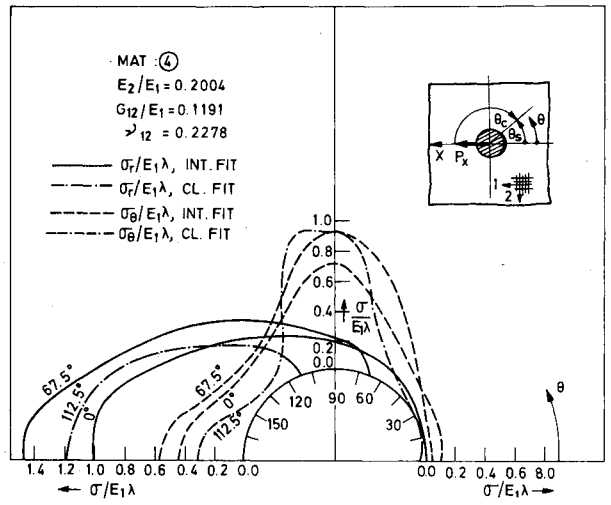

Fig. 4 Stress distribution on the hole boundary.

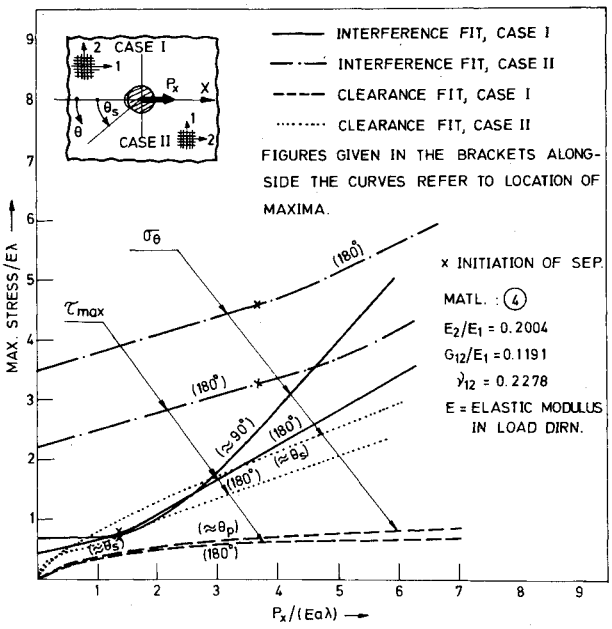

Fig. 5 Variation of maximum hoop tension and shear with load, interference and clearance fits.

Partial Contact

Partial contact is encountered at all loads in clearance fits and at loads greater than $(P_x)_{th}$ in interference fits. In this case, the extent of contact is specified by the angle θ_c. The boundary conditions [Eqs. (1b) and (1c)] can, in general, be satisfied by any of the several numerical techniques such as collocation, derivative collocation, least square collocation, successive integration of errors, etc.[19] With the present series form of complex potentials, even the simplest equidistant collocation has been found to lead to accurate estimates of the load and stresses.[18] The unknown load P_x and constants C_m are obtained as a solution to a system of simultaneous linear algebraic equations.

The following numerical scheme was used for collocation.

The half-interface $(0 \le \theta \le \pi)$ was divided into N divisions to give $N+1$ equidistant points for collocation. One of the collocation points was taken as the transition node between the separation and contact zones. For each configuration, solutions were obtained by successively halving the interval size, which gave suitable data for studying the convergence. To start with, the transition node was taken as $\theta = \pi$ and then successively shifted toward $\theta = 0$ so that solutions for various combinations of contact and separation were obtained. A positive value of $P_x/Ea\lambda$ indicates that for the given direction of load, λ is positive. This corresponds to an interference fit. Similarly, a negative value of $P_x/Ea\lambda$ would mean that the solution is obtained for a clearance fit $(\lambda < 0)$. The solution for push fit can be obtained by interpolation between values of $Ea\lambda/P_x$ that differ slightly from zero on either side.

Numerical Evaluation

The numerical calculations were made for orthotropic properties typical of FRC. Materials were labeled by numbers 1-5 conforming to the same materials used in Refs. 1 and 18, as listed in Table 1. In what follows, the materials are referred to by these numbers and their relevant properties are also mentioned in the tables and figures. A convergence study was first made to insure and check the accuracy. Further, the load contact behavior, stresses, and deformations were obtained for various materials.

Full Contact

The infinite system of equations (10) was solved for four sets of material properties. A convergence study was made by taking M successively as 8, 16, and 32. Table 2 gives the values for initiation of separation load $(P_x)_{th}/Ea\lambda$. As can be seen from the table, the convergence is very good, although slightly slower for materials with higher orthotropy. An 8 term solution has a maximum error of 3% and a 16 term solution is accurate within 0.001%.

Partial Contact

The numerical scheme as given in the last section was employed; the value of N was taken as 16, 32, and 64 for the study of convergence. The transition node was taken successively from $\theta_s = 0$ $(\theta_c = \pi)$ to $\theta_s = \pi$ $(\theta_c = 0)$ in the increments of $\pi/8$. Table 3 gives the values of $P_x/Ea\lambda$ for typical composites and for both cases I and II as the number of collocation intervals is successively doubled. The loads for $\theta_s = 0$ can be compared with initiation of separation loads obtained earlier from the full contact solutions (Table 2). The agreement is very good. The convergence of the collocation solution, as seen from Table 3, is very satisfactory. It is very good at low load levels but becomes slower at very large loads. A slight deterioration in convergence with higher orthotropy is also observed.

Figure 2 shows the errors in satisfying respective boundary conditions of contact and separation for material 5, obtained at the midcollocation points. The maximum error in σ_r is less than 1.2% of its maximum value and that in U is less than 3% of the maximum gap for $\theta_s = 22.5$ deg. Unlike in the plate load case,[1] the error does not increase with θ_s; at $\theta_s = 90$ deg, the errors are actually smaller as seen in the figure.

The load contact behavior of two orthotropic materials (3 and 4) for loading in both cases I and II is shown in Fig. 3. The case of isotropic material (material 1) is also shown for comparison. The stresses and displacements were evaluated for material 4. The distribution of $\sigma_r/E_1\lambda$ and $\sigma_\theta/E_1\lambda$ on the interface for various contact regions is shown in Fig. 4. Figure 5 shows the maximum hoop and shear stresses with increase of load. Figure 6a shows deformation of the hole boundary and Fig. 6b the variation of maximum displacements with the load.

Discussion

Full Contact Regime and Initiation of Separation

In interference fits, the pin and the plate maintain their contact up to the threshold load $(P_x/Ea\lambda)_{th}$ after which separation comes into play. The threshold values of load obtained for some composites in Table 1 can be seen from the last two columns of Table 2. During the full contact regime,

Table 1 Materials and their elastic constants used in the present work

Material No.		E_1, GPa	E_2, GPa	G_{12}, GPa	ν_{12}	E_2/E_1	G_{12}/E_1
1	Isotropic	1.0	1.0	0.3846	0.3	1.0	0.3846
2	Nearly isotropic	1.0	1.0	0.3800	0.3	1.0	0.3800
3	E-glass-epoxy (30% epoxy by volume)	49.58	18.16	9.12	0.2466	0.3663	0.1839
4	Boron-epoxy (30% by volume)	276.09	55.32	32.89	0.2278	0.2004	0.1191
5	Boron-epoxy (60% epoxy by volume)	159.16	21.88	15.27	0.2601	0.1375	0.0959

Table 2 Convergence of solution of infinite system of equations at the initiation of separation (values given are of $P_x/Ea\lambda$, E – elastic modulus in the load direction)

Material No.	Properties E_2/E_1	G_{12}/E_1	ν_{12}	Direction of load, P_x	No. of terms 8	16	32
2	1.000	0.380	0.300	Along E_1 or E_2	2.402	2.402	2.402
3	0.366	0.184	0.247	E_1	1.632	1.623	1.623
				E_2	3.152	3.168	3.168
4	0.200	0.119	0.228	E_1	1.283	1.258	1.258
				E_2	3.598	3.667	3.667
5	0.137	0.096	0.260	E_1	1.135	1.093	1.093
				E_2	3.956	4.095	4.095

the stresses and displacements vary linearly with load. The linear part of the curves at low loads in Fig. 5 shows the variation of maximum stress with load during this full contact regime. The stresses at zero load are the stresses due to interference only. The maximum hoop stress occurs on the Y axis.

Partial Contact Regime

At loads greater than the threshold loads in an interference fit, the contact is only partial and recedes nonlinearly with load. In a clearance fit, the contact starting at an infinitesimally small load builds up nonlinearly with load. This behavior, similar to that for the plate load,[1] is shown in Fig. 3, where both $P_x/Ea\lambda$ (broken lines) and its reciprocal $Ea\lambda/P_x$ (solid lines) are shown. The spread of separation in an interference fit and the spread of contact in a clearance fit is initially rapid, but becomes slower with increasing load. Both the spread of separation and the spread of contact reach asymptotic limiting values as the load is increased indefinitely. The limiting configuration is the same for both. The limiting values of θ_c or θ_s can be clearly obtained from $Ea\lambda/P_x$ curves at their intersection with the θ_c axis. This also corresponds to $\lambda=0$, the case of a push fit. It is clearly seen that in a push fit the angle of separation will be θ_p at all loads; this accounts for the linear variation of stresses and deformations with load in a push fit.

Effect of Orthotropy

Figure 3 shows the load-contact behavior of two composites (materials 3 and 4) and of an isotropic material (material 1) for both case I and II types of loading. From the variation of $P_x/Ea\lambda$ (where E is the modulus in the loaded direction), it is seen that stiffening the material along the loaded direction requires a higher load for the same spread of separation in an interference fit or for the same spread of contact in a clearance fit. The effect of stiffening the material along the direction transverse to the loaded direction is seen by comparing the curves for materials 4 to 3 to 1 for case I and for materials 1 to 3 to 4 for case II (in that order). It is seen that even for transverse stiffening, a higher load is required for the same spread of separation (contact) in interference (clearance) fits.

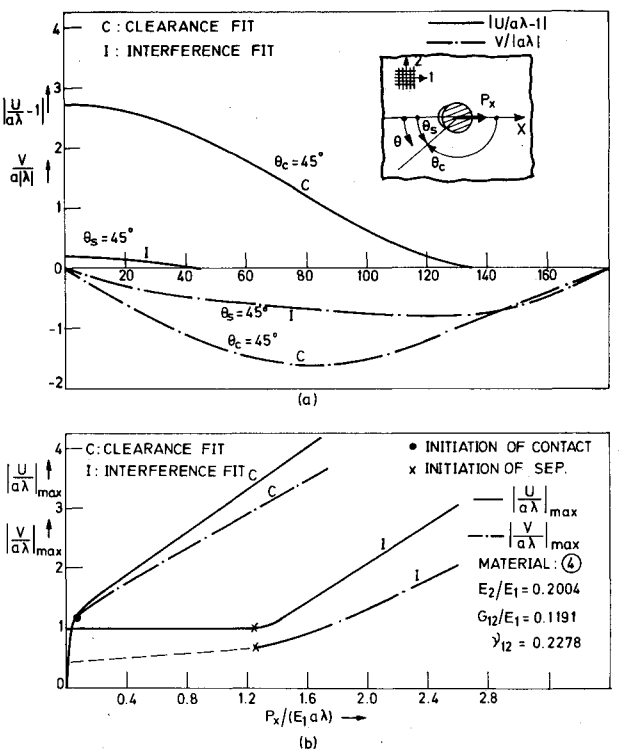

Fig. 6 Displacements at hole boundary, interference and clearance fits, pin load P_x along stiffer axis.

Stresses and Displacements

The radial pressure σ_r and the hoop stress σ_θ are distributed along the hole boundary as shown in Fig. 4 for the case of a typical boron-epoxy composite (material 4). Since the bearing strengths of composites are generally not to the same standard as their other properties, more accurate estimates of σ_r based on partial contact analysis should help to design better pin joints in composites. This is well illustrated by the following example.

Table 3 Convergence of solution by collocation studied by successively halving the mesh size (values given are of $P_x/Ea\lambda$, E = elastic modulus in load direction, θ_s = angle of separation)

		Load in stiffer direction			Load in weaker direction		
Material	θ_s	$M=$ 8	16	32	8	16	32
Material 4							
$E_2/E_1=0.200$	0.0	1.258	1.258	1.258	3.670	3.667	3.667
$G_{12}/E_1=0.119$	22.5	1.316	1.305	1.301	3.898	3.860	3.842
$\nu_{12}=0.228$	45.0	1.478	1.454	1.442	4.574	4.472	4.425
	67.5	2.021	1.932	1.891	6.637	6.272	6.111
	90.0	11.740	7.300	6.152	80.619	31.941	24.830
	112.5	−1.098	−1.291	−1.410	−2.881	−3.412	−3.730
	135.0	−0.250	−0.287	−0.308	−0.633	−0.737	−0.793
	157.5	−0.039	−0.052	−0.059	−0.095	−0.126	−0.143
	180.0	0.0	0.0	0.0	0.0	0.0	0.0
Material 3							
$E_2/E_1=0.366$	0.0	1.623	1.623	1.623	3.168	3.168	3.168
$G_{12}/E_1=0.184$	22.5	1.704	1.690	1.684	3.359	3.327	3.312
$\nu_{12}=0.247$	45.0	1.927	1.893	1.878	3.907	3.824	3.786
	67.5	2.649	2.530	2.475	5.576	5.286	5.157
	90.0	15.946	9.725	8.156	51.148	24.420	19.521
	112.5	−1.403	−1.654	−1.807	−2.557	−3.027	−3.310
	135.0	−0.316	−0.364	−0.391	−0.564	−0.656	−0.705
	157.5	−0.049	−0.065	−0.074	−0.085	−0.113	−0.128
	180.0	0.0	0.0	0.0	0.0	0.0	0.0

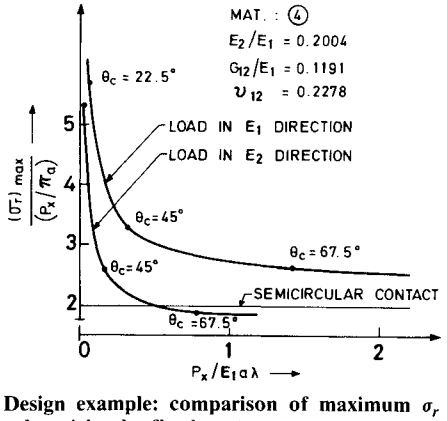

Fig. 7 Design example: comparison of maximum σ_r with partial contact and semicircular fixed contact.

The current design practice assumes stresses based on the assumption of a semicircular contact area and a cosine distribution of radial pressure. The maximum σ_r predicted by this method is $2P_x/\pi a$ at all loads (see Fig. 7). Based on our analysis of partial contact we see that $\sigma_{r\max}$ should vary nonlinearly with P_x. Figure 7 shows this variation of $\sigma_r/(P_x/\pi a)$ with P_x as obtained for material 4. It can be seen that there is a large difference between the values of σ_r predicted by semicircular contact theory and the present analysis. This difference becomes less as the configuration of contact approaches the limiting configuration of the push fit.

Figure 5 shows the variation of maximum hoop stress and maximum shear stress ($\tau_{\max}=\frac{1}{2}|\sigma_r-\sigma_\theta|$) with load P_x. The nonlinearity in the increase of stress with load is predominant at the initiation of separation or contact and fades out at higher loads. The locations of maximum stress change with magnitude of load for some combinations of material properties and load. The most likely locations are $\theta=0$, $\pi/2$, and θ_c. These form the potential locations for crack initiation in fatigue loading.

The distribution of the radial and tangential displacements along the hole boundary for some angles of separation are given in Fig. 6a. Figure 6b shows the increase in the maximum displacements with load giving an estimate of the flexibility of the joint. The advent of separation in the interference fits significantly increases the flexibility of the joint. Similarly, the increase in the tangential displacement rate with load (dV/dP_x) on separation suggests that fretting might increase at higher loads in interference fits with some friction.

Conclusion

A simple and efficient method to estimate accurately the stresses and deformations in pin-loaded holes in composites is developed. The method takes into account the partial contact of the pin over the hole periphery and satisfies all the boundary conditions of the contact and separation zones. A unified approach encompassing all types of fits is taken. An inverse formulation is used that seeks to obtain loads for a given configuration of contact.

The load-contact relationships and stresses and displacements are obtained for typical composites. The effect of orthotropy, load direction, and type of fit is studied. The technique and the results are of direct relevance to the analysis of pin joints in composites. The study of the partial contact should lead to improved estimates of stresses around holes for use in design of such joints for composites.

Acknowledgments

The author thanks Dr. B. Dattaguru of the Department of Aerospace Engineering, Indian Institute of Science, for his guidance and help during the course of this work. Thanks are also due to Prof. A. K. Rao and Dr. T. S. Ramamurthy of the same department for many helpful discussions. The financial support received under a Grants-in-Aid scheme from the Aeronautics Research and Development Board, Directorate of Aeronautics, New Delhi, is gratefully acknowledged.

References

[1] Mangalgiri, P.D. and Dattaguru, B., "Unbonded Smooth Rigid Pin in a Large Orthotropic Plate," to be published in *Res Mechanica*.

[2] Noble, B. and Hussain, M.A., "Exact Solution of Certain Dual Series for Indentation and Inclusion Problems," *International Journal of Engineering Science*, Vol. 7, 1969, pp. 1149-1161.

[3] Theocaris, P.S., "The Stress Distribution in a Strip Loaded in Tension by Means of a Central Pin," *Journal of Applied Mechanics*, Vol. 23, 1956, pp. 85-90.

[4]Wilson, H.B. Jr., "Approximate Determination of Contact Stresses in an Infinite Plate with a Smooth Circular Insert," *Developments in Theoretical and Applied Mechanics,* Vol. 2, edited by W.A. Shaw, Pergamon Press, New York, 1965, pp. 147-163.

[5]Sheremet'ev, M.P., "The Solution of the Equations of Certain Contact Problems of the Theory of Elasticity," *Problems of Continuum Mechanics,* edited by J.R.M. Radok, SIAM, 1961, pp. 419-439.

[6]Eshwar, V.A., Dattaguru, B., and Rao, A.K., "Partial Contact and Friction in Pin Joints," Aeronautical Research and Development Board, Govt. of India, New Delhi, Rept. ARDB-STR-5010, Dec. 1977.

[7]Rao, A.K., "Elastic Analysis of Pin Joints," *Computers and Structures,* Vol. 9, 1978, pp. 125-144.

[8]Ghosh, S.P., "Analysis of Joints with Elastic Pins," Ph.D. Thesis, Indian Institute of Science, Bangalore, 1978.

[9]Ghosh, S.P., Dattaguru, B., and Rao, A.K., "Load Transfer from a Smooth Elastic Pin to a Large Sheet," *AIAA Journal,* Vol. 19, May 1981, pp. 619-625.

[10]Eshwar, V.A., "Analysis of Clearance Fit Pin Joints," *International Journal of Mechanical Sciences,* Vol. 20, 1978, pp. 477-484.

[11]Eshwar, V.A., Dattaguru, B., and Rao, A.K., "Partial Loss of Contact in Interference Fit Pin Joints," *The Aeronautical Journal of the Royal Society,* 1979, pp. 233-237.

[12]Rao, A.K., Eshwar, V.A., and Dattaguru, B., "A Comprehensive Study of Interference and Clearance Fit Pins in Large Plates," *Mechanics Research Communications,* Vol. 4, 1977, pp. 325-332.

[13]Green, A.E., "Stress Systems in Aelotropic Plates, VII" *Proceedings of the Royal Society of London,* Vol. A184, 1945, pp. 301-345.

[14]De'Jong, T., "Stresses Around Pin-Loaded Holes in Elastically Orthotropic or Isotropic Plates," *Journal of Composite Materials,* Vol. 11, 1977, pp. 313-331.

[15]Oplinger, D.W. and Gandhi, K.R., "Analytical Studies of Structural Performance in Mechanically Fastened Composite Plates," Army Materials and Mechanics Research Center, Watertown, Mass., Rept. MS 74-8, 1974, pp. 221-240.

[16]Oplinger, D.W. and Gandhi, K.R., "Stresses in Mechanically Fastened Orthotropic Laminates," Paper presented at 2nd Conference of Fibrous Composites in Flight Vehicle Design, Ohio, May 1974.

[17]Lekhnitskii, S.G., *Anisotropic Plates,* translated from Russian by S.W. Tsai and T. Cheron, Gordon & Breach Science Publishers, New York, 1968.

[18]Mangalgiri, P.D. and Dattaguru, B., "Elastic Analysis of Pin Joints in Composite Plates," Aeronautics Research and Development Board, Govt. of India, New Delhi, Rept. ARDB-STR-5014, Nov. 1980.

[19]Collatz, L., *The Numerical Treatment of Differential Equations,* 3rd ed., Springer-Verlag, New York, 1960.